CLEO CONF 98-09
ICHEP98 860

Update on the Branching Fraction of $B \to \eta' K$

CLEO Collaboration

(July 21, 1998)

Abstract

Using a data sample of nearly 6 million $B\overline{B}$ pairs collected at CESR with the CLEO II/II.V detector, we revisit the decays $B^+ \to \eta' K^+$, $B^0 \to \eta' K^0$ and $B^+ \to \eta' \pi^+$. Using 80% more data than in previous studies, we confirm our previous observations of the decays $B^+ \to \eta' K^+$ and $B^0 \to \eta' K^0$. We measure branching fractions of $\mathcal{B}(B^+ \to \eta' K^+) = (7.4^{+0.8}_{-1.3} \pm 0.9) \times 10^{-5}$ and $\mathcal{B}(B^0 \to \eta' K^0) = (5.9^{+1.8}_{-1.6} \pm 0.9) \times 10^{-5}$. We set an upper limit for the decay $B^+ \to \eta' \pi^+$, $\mathcal{B}(B^+ \to \eta' \pi^+) < 1.2 \times 10^{-5}$.

B. H. Behrens,[1] W. T. Ford,[1] A. Gritsan,[1] H. Krieg,[1] J. Roy,[1] J. G. Smith,[1]
J. P. Alexander,[2] R. Baker,[2] C. Bebek,[2] B. E. Berger,[2] K. Berkelman,[2] V. Boisvert,[2]
D. G. Cassel,[2] D. S. Crowcroft,[2] M. Dickson,[2] S. von Dombrowski,[2] P. S. Drell,[2]
K. M. Ecklund,[2] R. Ehrlich,[2] A. D. Foland,[2] P. Gaidarev,[2] R. S. Galik,[2] L. Gibbons,[2]
B. Gittelman,[2] S. W. Gray,[2] D. L. Hartill,[2] B. K. Heltsley,[2] P. I. Hopman,[2]
J. Kandaswamy,[2] D. L. Kreinick,[2] T. Lee,[2] Y. Liu,[2] N. B. Mistry,[2] C. R. Ng,[2]
E. Nordberg,[2] M. Ogg,[2,*] J. R. Patterson,[2] D. Peterson,[2] D. Riley,[2] A. Soffer,[2]
B. Valant-Spaight,[2] A. Warburton,[2] C. Ward,[2] M. Athanas,[3] P. Avery,[3] C. D. Jones,[3]
M. Lohner,[3] C. Prescott,[3] A. I. Rubiera,[3] J. Yelton,[3] J. Zheng,[3] G. Brandenburg,[4]
R. A. Briere,[4] A. Ershov,[4] Y. S. Gao,[4] D. Y.-J. Kim,[4] R. Wilson,[4] H. Yamamoto,[4]
T. E. Browder,[5] Y. Li,[5] J. L. Rodriguez,[5] S. K. Sahu,[5] T. Bergfeld,[6] B. I. Eisenstein,[6]
J. Ernst,[6] G. E. Gladding,[6] G. D. Gollin,[6] R. M. Hans,[6] E. Johnson,[6] I. Karliner,[6]
M. A. Marsh,[6] M. Palmer,[6] M. Selen,[6] J. J. Thaler,[6] K. W. Edwards,[7] A. Bellerive,[8]
R. Janicek,[8] P. M. Patel,[8] A. J. Sadoff,[9] R. Ammar,[10] P. Baringer,[10] A. Bean,[10]
D. Besson,[10] D. Coppage,[10] C. Darling,[10] R. Davis,[10] S. Kotov,[10] I. Kravchenko,[10]
N. Kwak,[10] L. Zhou,[10] S. Anderson,[11] Y. Kubota,[11] S. J. Lee,[11] R. Mahapatra,[11]
J. J. O'Neill,[11] R. Poling,[11] T. Riehle,[11] A. Smith,[11] M. S. Alam,[12] S. B. Athar,[12] Z. Ling,[12]
A. H. Mahmood,[12] S. Timm,[12] F. Wappler,[12] A. Anastassov,[13] J. E. Duboscq,[13]
K. K. Gan,[13] T. Hart,[13] K. Honscheid,[13] H. Kagan,[13] R. Kass,[13] J. Lee,[13] H. Schwarthoff,[13]
A. Wolf,[13] M. M. Zoeller,[13] S. J. Richichi,[14] H. Severini,[14] P. Skubic,[14] A. Undrus,[14]
M. Bishai,[15] S. Chen,[15] J. Fast,[15] J. W. Hinson,[15] N. Menon,[15] D. H. Miller,[15]
E. I. Shibata,[15] I. P. J. Shipsey,[15] S. Glenn,[16] Y. Kwon,[16,†] A.L. Lyon,[16] S. Roberts,[16]
E. H. Thorndike,[16] C. P. Jessop,[17] K. Lingel,[17] H. Marsiske,[17] M. L. Perl,[17] V. Savinov,[17]
D. Ugolini,[17] X. Zhou,[17] T. E. Coan,[18] V. Fadeyev,[18] I. Korolkov,[18] Y. Maravin,[18]
I. Narsky,[18] R. Stroynowski,[18] J. Ye,[18] T. Wlodek,[18] M. Artuso,[19] E. Dambasuren,[19]
S. Kopp,[19] G. C. Moneti,[19] R. Mountain,[19] S. Schuh,[19] T. Skwarnicki,[19] S. Stone,[19]
A. Titov,[19] G. Viehhauser,[19] J.C. Wang,[19] J. Bartelt,[20] S. E. Csorna,[20] K. W. McLean,[20]
S. Marka,[20] Z. Xu,[20] R. Godang,[21] K. Kinoshita,[21] I. C. Lai,[21] P. Pomianowski,[21]
S. Schrenk,[21] G. Bonvicini,[22] D. Cinabro,[22] R. Greene,[22] L. P. Perera,[22] G. J. Zhou,[22]
S. Chan,[23] G. Eigen,[23] E. Lipeles,[23] J. S. Miller,[23] M. Schmidtler,[23] A. Shapiro,[23]
W. M. Sun,[23] J. Urheim,[23] A. J. Weinstein,[23] F. Würthwein,[23] D. E. Jaffe,[24] G. Masek,[24]
H. P. Paar,[24] E. M. Potter,[24] S. Prell,[24] V. Sharma,[24] D. M. Asner,[25] J. Gronberg,[25]
T. S. Hill,[25] D. J. Lange,[25] R. J. Morrison,[25] T. K. Nelson,[25] and D. Roberts[25]

[1]University of Colorado, Boulder, Colorado 80309-0390
[2]Cornell University, Ithaca, New York 14853
[3]University of Florida, Gainesville, Florida 32611
[4]Harvard University, Cambridge, Massachusetts 02138
[5]University of Hawaii at Manoa, Honolulu, Hawaii 96822
[6]University of Illinois, Urbana-Champaign, Illinois 61801

[*]Permanent address: University of Texas, Austin TX 78712.

[†]Permanent address: Yonsei University, Seoul 120-749, Korea.

[7]Carleton University, Ottawa, Ontario, Canada K1S 5B6
and the Institute of Particle Physics, Canada
[8]McGill University, Montréal, Québec, Canada H3A 2T8
and the Institute of Particle Physics, Canada
[9]Ithaca College, Ithaca, New York 14850
[10]University of Kansas, Lawrence, Kansas 66045
[11]University of Minnesota, Minneapolis, Minnesota 55455
[12]State University of New York at Albany, Albany, New York 12222
[13]Ohio State University, Columbus, Ohio 43210
[14]University of Oklahoma, Norman, Oklahoma 73019
[15]Purdue University, West Lafayette, Indiana 47907
[16]University of Rochester, Rochester, New York 14627
[17]Stanford Linear Accelerator Center, Stanford University, Stanford, California 94309
[18]Southern Methodist University, Dallas, Texas 75275
[19]Syracuse University, Syracuse, New York 13244
[20]Vanderbilt University, Nashville, Tennessee 37235
[21]Virginia Polytechnic Institute and State University, Blacksburg, Virginia 24061
[22]Wayne State University, Detroit, Michigan 48202
[23]California Institute of Technology, Pasadena, California 91125
[24]University of California, San Diego, La Jolla, California 92093
[25]University of California, Santa Barbara, California 93106

I. INTRODUCTION

The first observation of the decay $B^+ \to \eta' K^+$ (charge conjugate modes are implied) was reported by CLEO in January of 1997 [1]. This decay mode was already of interest because the decay amplitude is expected to be dominated by the $b \to s$ "gluonic penguin" diagram shown in Fig. 1a and b. More interesting, however, was that the branching fraction was unexpectedly large. The preliminary result was 7.8×10^{-5}, with large errors. This was more than a factor of three larger than previous theoretical expectations [2] and five times larger than the branching fraction of the other measured gluonic penguin decay, $B^0 \to K^+\pi^-$. This surprising result, along with the large rate for the inclusive decay $B \to \eta' X_s$ [3], set off a flurry of theoretical activity which continues to this day.

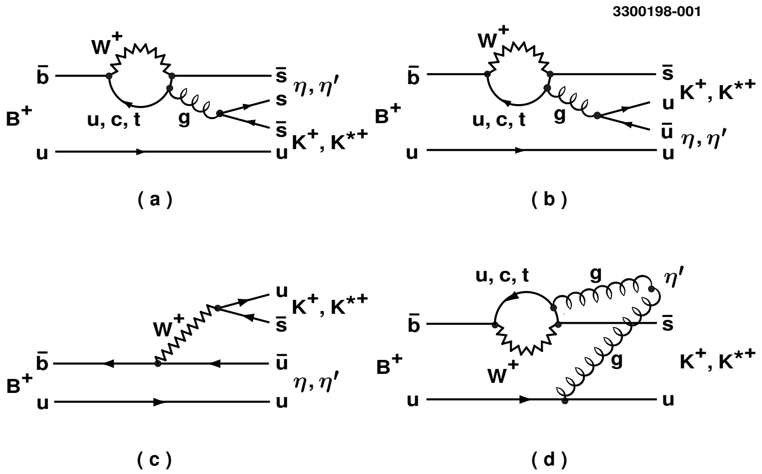

FIG. 1. Feynman diagrams relevant to the decay $B^+ \to \eta' K^+$. The $B^0 \to \eta' K^0$ diagrams are similar, with a d spectator quark.

It has been known for many years that the rate for $B^+ \to \eta' K^+$ should be large compared with $B^+ \to \eta K^+$ due to interference effects between the two penguin diagrams (Fig. 1a and b) [4]. However this effect was included in the early predictions which were far below the measured rate. One possible explanation for the enhanced rate is added contributions from the QCD gluon anomaly or other flavor singlet processes (Fig. 1d) [5]. Others have suggested η_c-η' mixing, final state rescattering, "charming penguins," and modifications to model parameters such as form factors [6].

An upward statistical fluctuation was another possibility since the measurement uncertainty was quite large. In fact, in our most recent publication [7] the measured branching fraction dropped to $(6.5^{+1.5}_{-1.4} \pm 0.9) \times 10^{-5}$. This result includes the $\eta' \to \rho^0\gamma$ and $\eta' \to \pi^+\pi^-\eta$ with $\eta \to \pi^+\pi^-\pi^0$ decay modes in addition to the original $\eta' \to \pi^+\pi^-\eta$ with $\eta \to \gamma\gamma$ decay mode. In this paper we revisit the $B^+ \to \eta' K^+$ decay with 80% more data, studying the highest efficiency decay modes ($\eta' \to \rho^0\gamma$ and $\eta' \to \pi^+\pi^-\eta$ with $\eta \to \gamma\gamma$), to determine the branching fraction with reduced uncertainty. We also revisit the decay $B^0 \to \eta' K^0$, which we previously observed to have a slightly smaller but statistically consistent branching fraction, $(4.7^{+2.7}_{-2.0} \pm 0.9) \times 10^{-5}$ [7].

II. DATA SAMPLE AND INITIAL EVENT SELECTION

The results presented here are based on 5.6 fb^{-1} of data taken on the $\Upsilon(4S)$ resonance and 2.9 fb^{-1} taken slightly below the resonance. The on-resonance data sample contains 5.8×10^6 $B\overline{B}$ pairs. The data were collected with the CLEO II [8] and CLEO II.V [9] detectors, at the Cornell Electron Storage Ring (CESR). The detector elements most important for the analyses presented here are the tracking system, which is used to measure the momentum and energy loss rate (dE/dx) of charged particles, and the CsI crystal calorimeter, which is used to measure the energy of photons.

In 1995 the CLEO II detector was upgraded with the addition of a silicon vertex detector. The primary benefit of the silicon vertex detector for these analyses is in K_S reconstruction and background rejection. The drift chamber gas was also changed from argon-ethane to helium-propane, resulting in reduced multiple scattering and other improvements due to the smaller Lorentz angle. The momentum resolution and K–π separation (from dE/dx) at 2.6 GeV/c were both improved by $\sim$15%. The CLEO II data was also reprocessed with a variety of tracking and dE/dx improvements.

The data are analyzed with a maximum likelihood fit after selecting a subset of the data which contains candidate $B^+ \to \eta' K^+$, $B^+ \to \eta' \pi^+$, and $B^0 \to \eta' K^0$ decays. We reconstruct η' candidates in two decay channels, $\eta' \to \pi^+\pi^-\eta$ with $\eta \to \gamma\gamma$, and $\eta' \to \rho^0\gamma$ with $\rho^0 \to \pi^+\pi^-$. The K^0 in $B^0 \to \eta' K^0$ is observed through the $K_S \to \pi^+\pi^-$ decay.

In each event, we require the total number of charged tracks to be greater than four. Tracks used to reconstruct B mesons are required to pass selection criteria on the number of drift chamber measurements, goodness of fit, and consistency with an origin at the primary or secondary vertex. Charged tracks are also required to have momentum greater than 100 MeV/c. For charged pions used in secondary particle reconstruction, the measured value of dE/dx is required to be within three standard deviations (σ) of the expected value. Pairs of charged tracks used to reconstruct K_S's are required to have well measured displaced vertices. We also require that the K_S momentum vector is consistent with an origin at the beam spot.

Candidate photons must be isolated calorimeter clusters with photon-like spatial distribution and energy deposition exceeding 30 MeV. We exclude photon pairs from extremely asymmetric η decays to reject soft photon backgrounds. We require $|\cos\theta^*| < 0.97$, where θ^* is the η center-of-mass decay angle with respect to its flight direction. The momentum of the η is obtained from a kinematic fit to the photon momenta with the η mass constrained at its nominal value [10]. To reduce combinatoric background, the candidate η momentum is required to be greater than 100 MeV/c.

Electrons are rejected based on dE/dx and the ratio of the measured track momentum and the associated shower energy in the calorimeter. Muons are rejected by requiring that the track penetrate less than seven interaction lengths of material.

An event shape cut is used to suppress background from continuum $q\bar{q}$ events. Because the B mesons produced in $\Upsilon(4S)$ decays are almost at rest, the decay products of the $B\bar{B}$ pair tend to be spherically distributed. Particles from $q\bar{q}$ production tend to have a more jet-like distribution. We define the angle θ_T as the angle between the thrust axis of the charged particles and photons used to form the candidate B meson and the thrust axis of the remaining particles and photons in the event [11]. All events are required to have

$|\cos\theta_T| < 0.9$. In this variable, continuum background is strongly peaked near 1.0 while signal is approximately flat.

III. MAXIMUM LIKELIHOOD ANALYSES

A. INPUTS

The primary observable in this analysis is M, the beam-constrained B mass. Each B meson must have energy equal to the energy of one beam, $E_{\rm beam}$. Since we know the beam energy with higher accuracy than we can measure the energy of the B meson, we calculate the B mass assuming its energy is equal to $E_{\rm beam}$: $M = \sqrt{E^2_{\rm beam} - p^2_B}$, where p_B is the measured momentum of the B candidate. The beam-constrained B mass has a typical resolution of 2.7 MeV/c^2.

Another important quantity, ΔE, measures the difference between the measured B energy (E_B) and $E_{\rm beam}$ ($\Delta E = E_B - E_{\rm beam}$). The resolution in ΔE is typically about 30 MeV. ΔE should peak at 0 (44 MeV) for $\eta' K$ ($\eta'\pi$) signal, and have a linearly falling distribution for continuum background.

An event shape variable is also included in the likelihood fit. A Fisher discriminant ($\mathcal{F}$) is formed with 11 variables correlated with the event shape: the scalar momentum sum of charged particles and photons in nine cones of increasing polar angle around the thrust axis of the candidate, the angle between the thrust axis of the candidate and the beam axis, and the angle between the candidate B direction and the beam axis. This discriminant is described in detail in Ref. [12]. For this variable, signal peaks around 0.4 and background around 0.7. In each case, the low side of the distribution has a σ of ~ 0.13 and the high side ~ 0.17.

For the modes with $\eta' \to \rho^0\gamma$, we use the angle θ_h between the direction of the parent B meson and the direction of the charged decay products of the ρ, both calculated in the rest frame of the ρ. We expect signal to have a distribution proportional to $\sin^2\theta_h$, while background is nearly flat.

Unbinned maximum likelihood fits are performed to obtain signal yields for the decay modes $B^+ \to \eta' K^+$, $B^+ \to \eta'\pi^+$, and $B^0 \to \eta' K^0$. For the modes $B^+ \to \eta' K^+$ and $B^+ \to \eta'\pi^+$, we perform a simultaneous fit. To resolve the ambiguity in the identity of the high-momentum charged track, we use the fact that ΔE is computed assuming that the charged track is a kaon. If the track is a pion, the distribution is shifted by +44 MeV. For these modes we also include the dE/dx information as input to the fit. The quantities used are

$$S_K = \frac{(dE/dx)_{\rm measured} - (dE/dx)_{\rm K\ hypothesis}}{\sigma_{\rm K}} \tag{1}$$

and

$$S_\pi = \frac{(dE/dx)_{\rm measured} - (dE/dx)_{\pi\ \rm hypothesis}}{\sigma_\pi}, \tag{2}$$

where $\sigma_{\rm K}(\sigma_\pi)$ is the expected resolution for kaons(pions). As for ΔE, $S_K(S_\pi)$ will have a distribution centered on zero for kaons(pions) and will be shifted for pions(kaons).

The quantities M, ΔE, $\mathcal{F}$, and $M_{\eta'}$ (the reconstructed invariant mass of the η' candidate) are used as input information to the fit in all cases. We also use as appropriate $\cos\theta_h$, dE/dx, and the reconstructed invariant masses of the η and K_S candidates (M_η and M_{K_S} respectively).

Before performing the likelihood fit, a number of preliminary cuts are applied to the fit variables. We require $|\Delta E| < 0.2$ GeV, $5.2 < M < 5.3$ GeV/c^2, $0.93 < M_{\eta'} < 0.99$ GeV/c^2, and, as required, $0.5 < M_\eta < 0.6$ GeV/c^2, $0.47 < M_{K_S} < 0.53$ GeV/c^2, and $0.4 < M_{\rho^0} < 0.95$ GeV/c^2.

B. METHOD

For N input events, the likelihood is defined as

$$\mathcal{L} = e^{-(N_S+N_B)} \prod_{i=1}^{N} \{N_S \mathcal{P}_S(f_1,...,f_m;x_i) + N_B \mathcal{P}_B(f_1,...,f_m;x_i)\}, \tag{3}$$

where $\mathcal{P}_S$ and $\mathcal{P}_B$ are the probabilities for event i with input quantities x_i and parameters f_j to be signal and continuum background, respectively. N_S and N_B, the free parameters of the fit, are the number of signal and continuum background events in the fitted data sample, respectively. The exponential factor preceding the product ensures that $N_S + N_B$ is equal to the total number of input events. For the simultaneous fit of $B^+ \to \eta' K^+$ and $B^+ \to \eta'\pi^+$, the likelihood is defined as

$$\mathcal{L} = e^{-(N_S^\pi+N_S^K+N_B)} \prod_{i=1}^{N} \{N_S^\pi \mathcal{P}_S^\pi + N_S^K \mathcal{P}_S^K + N_B[f_B^K \mathcal{P}_B^K + (1-f_B^K)\mathcal{P}_B^\pi]\}, \tag{4}$$

where the π and K superscripts refer to the hypothesis made for the ambiguous charged track and f_B^K is the fraction of continuum background events for which the ambiguous charged track is a kaon. The latter is also a free parameter of the maximum likelihood fit.

The signal probability distribution functions ($\mathcal{P}_S$) are determined by fits to signal Monte Carlo. The background probability distribution functions ($\mathcal{P}_B$) are determined by fits to off-resonance and on-resonance "grand sideband" ($M < 5.27$ GeV/c^2) data. For M and $M_{\eta'}$ signal shapes, we use Gaussian functions; for ΔE, M_η, and M_{K_S} signal shapes we use double Gaussians; and for $\mathcal{F}$ and S_K signal and background shapes we use bifurcated Gaussians. For $M_{\eta'}$, M_η, and M_{K_S} background we use the sum of a first-degree polynomial and the signal shape to describe the pure combinatoric background and the component of real particles in the background. Finally, for ΔE the background is described by a first-degree polynomial and for M we use the empirical shape [13]

$$f(M) \propto M\sqrt{1-x^2}\, e^{-\xi(1-x^2)}, \tag{5}$$

where $x \equiv M/E_b$ and ξ is a fixed parameter for each decay mode.

C. RESULTS

Table I gives the results of the maximum likelihood analyses. Shown in the table are the efficiency(ϵ) for signal Monte Carlo events (excluding branching fractions) and the total efficiency($\epsilon_{\rm tot}$) (including relevant branching fractions) with its systematic error. Also included are the signal yields($N_{\rm sig}$), the statistical significance($\mathcal{S}$) of the yield in number of standard deviations, and the calculated branching fraction($\mathcal{B}$). The results of the two η' decay modes are combined by adding the $-2ln(\mathcal{L}/\mathcal{L}_{\rm max})$ distributions together. The statistical significance of the yield is defined by

$$\mathcal{S} = \sqrt{-2ln(\mathcal{L}_0/\mathcal{L}_{\rm max})}, \tag{6}$$

where $\mathcal{L}_{\rm max}$ denotes the value of the likelihood function at the point of maximum likelihood, and $\mathcal{L}_0$ denotes the value of the likelihood function at zero yield. The first error on the quoted branching fractions is statistical and the second systematic. The systematic error includes a contribution from the efficiency and a contribution from changes in fit yield that depend on variations in the parameters of the probability distribution functions.

The 90% confidence level upper limit on the yield is determined by finding the point at which the integral of the likelihood curve is at 90% of its total. To take efficiency systematic errors into account, we reduce the efficiency by 12% (one standard deviation) before calculating the upper limit.

TABLE I. Results from maximum likelihood analyses. Branching fraction upper limits are at the 90% confidence level. The statistical significance is given in standard deviation units. Numbers in bold face are found by combining the results for the two η' decay modes.

Mode	ϵ(%)	$\epsilon_{\rm tot}$(%)	$N_{\rm sig}$	$\mathcal{S}$	$\mathcal{B}(\times 10^{-5})$
$\eta' K^+$	-	-	-	12.7	$\mathbf{7.4^{+0.8}_{-1.3} \pm 1.0}$
$(\eta' \to \pi^+\pi^-\eta)$	29	5.0 ± 0.6	18.4	8.9	$6.3^{+1.7}_{-1.5} \pm 0.8$
$(\eta' \to \rho^0\gamma)$	36	10.8 ± 1.4	50.2	9.0	$7.8^{+1.5}_{-1.4} \pm 1.0$
$\eta' K^0$	-	-	-	7.3	$\mathbf{5.9^{+1.8}_{-1.6} \pm 0.9}$
$(\eta' \to \pi^+\pi^-\eta)$	28	1.6 ± 0.2	5.4	5.4	$5.4^{+2.8}_{-2.1} \pm 0.9$
$(\eta' \to \rho^0\gamma)$	33	3.4 ± 0.5	12.7	4.9	$6.3^{+2.5}_{-2.1} \pm 0.8$
$\eta' \pi^+$	-	-	-	-	$\mathbf{< 1.2}$
$(\eta' \to \pi^+\pi^-\eta)$	29	5.0 ± 0.6	1.0	1.0	< 1.8
$(\eta' \to \rho^0\gamma)$	36	10.7 ± 1.2	0.0	0.0	< 1.5

Fig. 2 shows the maximum likelihood contours in 2σ increments for $B^+ \to \eta' K^+$ and $B^+ \to \eta' \pi^+$. The statistical significance of the $B^+ \to \eta' K^+$ signal is 12.7σ. Fig. 3 shows projections of M and ΔE for the $B^+ \to \eta' K^+$ decay mode. In the upper two plots, the η' decay proceeds through $\eta' \to \pi^+\pi^-\eta$. In the lower two plots the η' decay proceeds through $\eta' \to \rho^0\gamma$. Note that for the data histograms, cuts are applied to all of the likelihood fit input quantities except the one plotted. The likelihood fit curves overlaid on the data are not a fit to the data shown but rather show the overall fit, scaled to account for the additional cuts. Fig. 4 shows the value of $-2\ln(\mathcal{L}/\mathcal{L}_{\rm max})$ as a function of the branching fraction for the two $B^0 \to \eta' K^0$ analyses individually and in combination. The minimum of the solid curve corresponds to the combined branching fraction quoted in Table I. Fig. 5 shows the projections of M and ΔE for $B^0 \to \eta' K^0$. Again, cuts have been applied to quantities other than the one plotted before making the projection.

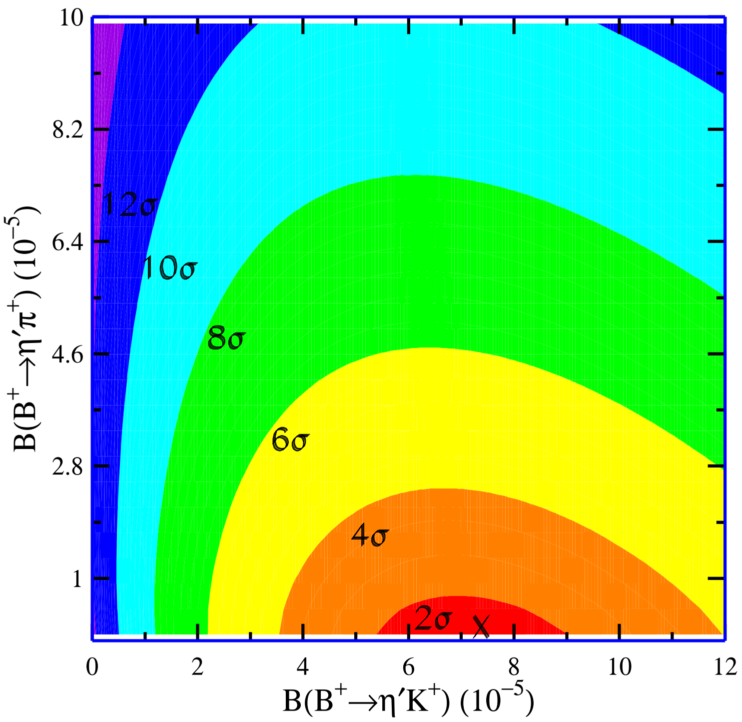

FIG. 2. Plot of maximum likelihood fit contours as a function of the $B^+ \to \eta' K^+$ and $B^+ \to \eta' \pi^+$ branching fractions, in 2σ increments.

IV. CONCLUSIONS AND DISCUSSION

We have studied the decays $B^+ \to \eta' K^+$, and $B^0 \to \eta' K^0$ using a data sample 80% larger than in previous studies. We find large signals in both modes, consistent with our previous results. An unbinned maximum-likelihood analysis finds a 12.7σ excess for the mode $B^+ \to \eta' K^+$, with a branching fraction $\mathcal{B}(B^+ \to \eta' K^+) = (7.4^{+0.8}_{-1.3} \pm 0.9) \times 10^{-5}$. We also observe the decay $B^0 \to \eta' K^0$, with a branching fraction of $\mathcal{B}(B^0 \to \eta' K^0) = (5.9^{+1.8}_{-1.6} \pm 0.9) \times 10^{-5}$ and a statistical significance of 7.3σ. Both of these branching fraction measurements have increased with added data, suggesting that our original results were not an upward statistical fluctuation. We do not see a signal in the decay mode $B^+ \to \eta' \pi^+$. We set an upper limit of $\mathcal{B}(B^+ \to \eta' \pi^+) < 1.2 \times 10^{-5}$ at the 90% confidence level.

The results for $B^+ \to \eta' K^+$ are larger than most theoretical predictions. While some theorists conclude that variations (perhaps improbable) in the theoretical parameters can account for the large rate [14], others find considerable difficulty in accounting for such a

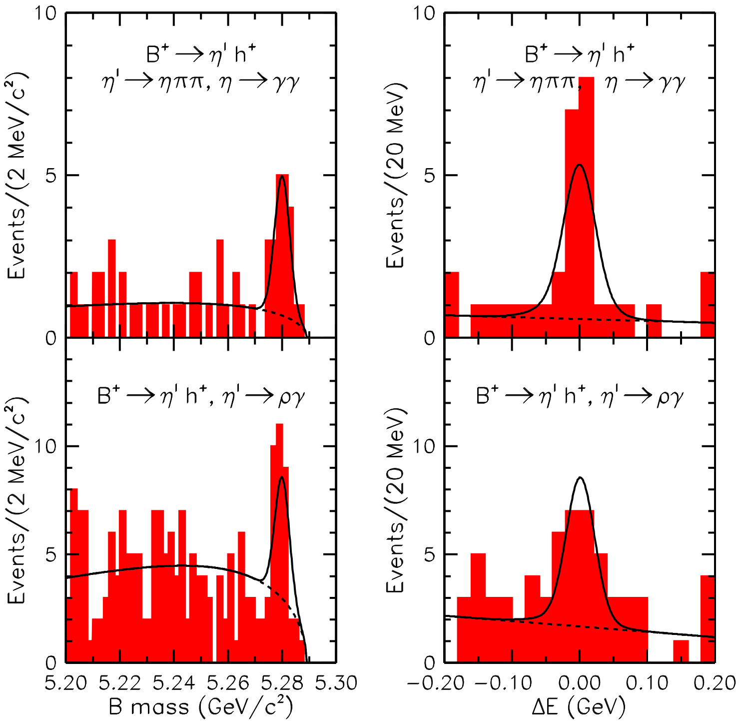

FIG. 3. Projections of the variables M and ΔE for the decay $B^+ \to \eta' K^+/\ \pi^+$. $B^+ \to \eta'\pi^+$ events would appear at +0.044 GeV in the ΔE plot. For these histograms, cuts are applied to the other variables used in the fits and the normalization of the likelihood fits are scaled accordingly. The upper two plots correspond to the η' decay $\eta' \to \pi^+\pi^-\eta$ while the lower two plots correspond to the η' decay $\eta' \to \rho^0\gamma$.

large rate. For instance a recent comprehensive calculation by Ali, Kramer and Lü [15] finds a likely range of $(2\text{–}4)\times 10^{-5}$. The results for the charged and neutral B decays are in good agreement, as expected since the two modes have the same dominant diagrams with the only difference being the flavor of the spectator quark.

A recent sum rule derived by Lipkin [16] suggests that the increased rate is not due to final-state interactions. Neglecting only electroweak penguins (not shown) and "hairpin" diagrams (Fig. 1d), both expected to be small, he derives the sum rule

$$\mathcal{B}(B^+ \to \eta' K^+) + \mathcal{B}(B^+ \to \eta K^+) = \mathcal{B}(B^+ \to K^+\pi^0) + \mathcal{B}(B^+ \to K^0\pi^+)\,. \tag{7}$$

Neglecting $B^+ \to \eta K^+$, for which there is only a limit ($< 1.4 \times 10^{-5}$) at present, we find that the left-hand side of the equation is $(7.4^{+1.3}_{-1.6}) \times 10^{-5}$; taking numbers from CLEO results submitted to this conference [17], the right-hand side is $(2.9 \pm 0.7) \times 10^{-5}$. It would appear that this sum rule is violated, indicating the importance of other effects such as hairpin diagrams (Fig. 1d) or larger η_c-η' mixing than has been calculated recently [18].

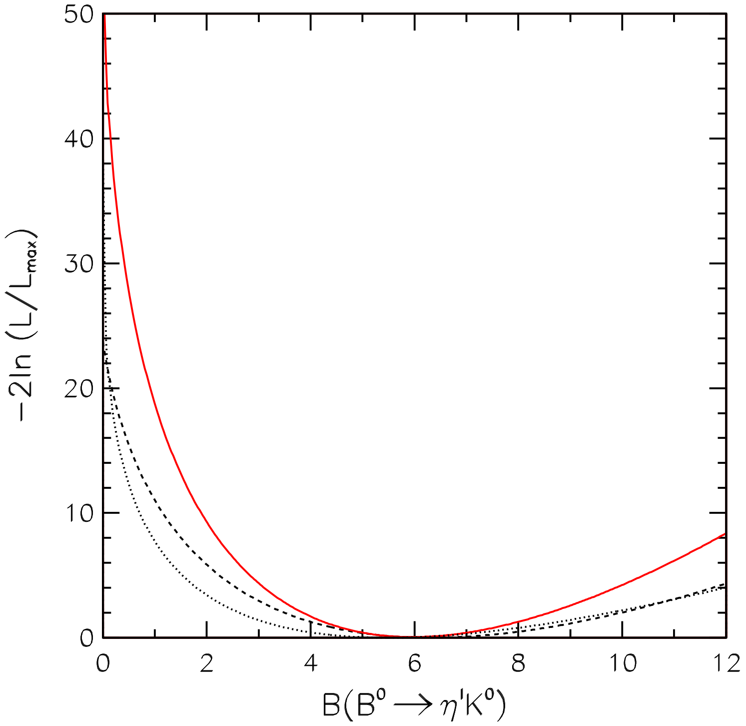

FIG. 4. Plot of $-2\ln(\mathcal{L}/\mathcal{L}_{\rm max})$ as a function of the $B^0 \to \eta' K^0$ branching fraction. The dotted line corresponds to the η' decay $\eta' \to \pi^+\pi^-\eta$ and the dashed line corresponds to the η' decay $\eta' \to \rho^0\gamma$. The solid line is the result for the two modes combined.

V. ACKNOWLEDGMENTS

We gratefully acknowledge the effort of the CESR staff in providing us with excellent luminosity and running conditions. We thank A. Ali, H-Y. Cheng, H. Lipkin, and A. Soni for useful discussions. J.R. Patterson and I.P.J. Shipsey thank the NYI program of the NSF, M. Selen thanks the PFF program of the NSF, M. Selen and H. Yamamoto thank the OJI program of DOE, J.R. Patterson, K. Honscheid, M. Selen and V. Sharma thank the A.P. Sloan Foundation, M. Selen and V. Sharma thank Research Corporation, S. von Dombrowski thanks the Swiss National Science Foundation, and H. Schwarthoff thanks the Alexander von Humboldt Stiftung for support. This work was supported by the National Science Foundation, the U.S. Department of Energy, and the Natural Sciences and Engineering Research Council of Canada.

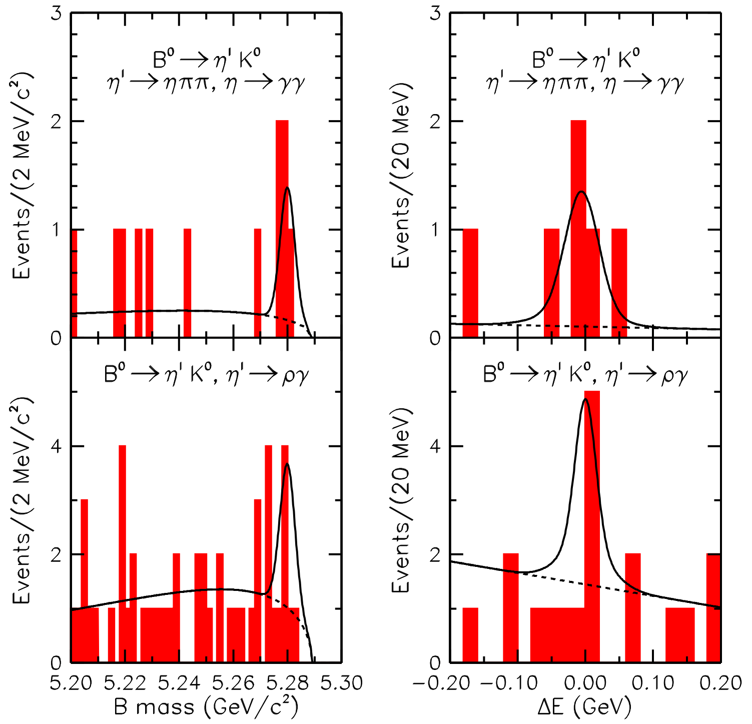

FIG. 5. Projections of the variables M and ΔE for the decay $B^0 \to \eta' K^0$. For these histograms, cuts are applied to the other variables used in the fits and the normalization of the likelihood fits are scaled accordingly. The upper two plots correspond to the decay $\eta' \to \pi^+\pi^-\eta$ while the lower two plots correspond to the decay $\eta' \to \rho^0\gamma$.

REFERENCES

[1] J.G. Smith, talk presented at the *1997 Aspen Winter Conference on Particle Physics*, Aspen, Colorado, January 1997.

[2] L-L. Chau, *et al.* Phys. Rev. D **43**, 2176 (1991), erratum Phys. Rev. D **58**, 019902 (1998); G. Kramer, W.F. Palmer, H. Simma, Z. Phys. C **66**, 429 (1995); D-S. Du, L. Guo, Z. Phys. C **75**, 9 (1997)

[3] T.E. Browder *et al.* (CLEO Collaboration), CLEO Report No. CLNS 98/1544, submitted to Phys. Rev. Lett.

[4] H.J. Lipkin, Phys. Lett. B **254**, 247 (1991).

[5] A.S. Dighe, M. Gronau and J.L. Rosner, Phys. Rev. Lett. **79** 4333, (1997); D. Atwood, A. Soni, Phys. Lett. B **405**, 150 (1997); M.R. Ahmady, E. Kou, A. Sugamoto, Phys. Rev. D **58**, 014015 (1998); D. Du, C.S. Kim and Y. Yang, Phys. Lett. B **426**, 133 (1998).

[6] I. Halperin, A. Zhitnitsky, Phys. Rev. D**56**, 7247 (1997), Phys. Rev. Lett. **80**, 438 (1998); H-Y. Cheng and B. Tseng, Phys. Lett. B **415**, 263 (1997); F. Yuan, K-T. Chao, Phys. Rev. D **56**, R2495 (1997); A. Datta, X-G. He, S. Pakvasa, Phys. Lett. B **419**, 369 (1998); A. Ali, C. Greub, Phys. Rev. D **57**, 2996 (1998); M. Ciuchini, *et al.* Nucl. Phys. **B512**, 3 (1998).

[7] B.H. Behrens, *et al.*, Phys. Rev. Lett. **80**, 3710 (1998).

[8] Y. Kubota *et al.* (CLEO Collaboration), Nucl. Instrum. Methods A **320**, 66 (1992).
[9] T. Hill, Vertex 97, Rio de Janeiro, Brazil (1997).
[10] Particle Data Group, R.M. Barnett *et al.*, Phys. Rev. D **54**, 1 (1996).
[11] E. Farhi, Phys. Rev. Lett. **39**, 1587 (1977).
[12] D.M. Asner *et al.* (CLEO Collaboration), Phys. Rev. D **53**, 1039 (1996).
[13] H. Albrecht *et al.* (ARGUS Collaboration), Phys. Lett. B **241**, 278 (1990), Phys. Lett. B **254**, 288 (1991).
[14] N.G. Deshpande, B. Dutta, S. Oh, Phys. Rev. D **57**, 5723 (1998).
[15] A. Ali, G. Kramer, C-D. Lü, Report No. DESY 98-041, hep-ph/9804363 (1998).
[16] H. Lipkin, Report No. ANL-HEP-CP-97-45A, hep-ph/9708253 (1997).
[17] M. Artuso *et al.* (CLEO Collaboration), CLEO CONF 98-20, ICHEP98-858 (1998).
[18] A. Ali, J. Chay, C. Greub, P. Ko, Phys. Lett. B **424**, 161 (1998); Th. Feldmann, P. Kroll, B. Stech, Report No. WU-B-98-2, hep-ph/9802409 (1998).